Nonlinear Dynamics (2005) 39: 349–367

Dynamic Stability Problems of Anisotropic Cylindrical Shells via a Simplified Analysis

EELCO L. JANSEN
Faculty of Aerospace Engineering, Delft University of Technology, Kluyverweg 1, 2629 HS Delft, The Netherlands
(e-mail: E.L.Jansen@LR.TUDelft.nl; fax: +31-15-2785337)

(Received: 1 May 2002; accepted: 11 August 2004)

Abstract. An analytical–numerical method involving a small number of generalized coordinates is presented for the analysis of the nonlinear vibration and dynamic stability behaviour of imperfect anisotropic cylindrical shells. Donnell-type governing equations are used and classical lamination theory is employed. The assumed deflection modes approximately satisfy 'simply supported' boundary conditions. The axisymmetric mode satisfying a relevant coupling condition with the linear, asymmetric mode is included in the assumed deflection function. The shell is statically loaded by axial compression, radial pressure and torsion. A two-mode imperfection model, consisting of an axisymmetric and an asymmetric mode, is used. The static-state response is assumed to be affine to the given imperfection. In order to find approximate solutions for the dynamic-state equations, Hamilton's principle is applied to derive a set of modal amplitude equations. The dynamic response is obtained via numerical time-integration of the set of nonlinear ordinary differential equations. The nonlinear behaviour under axial parametric excitation and the dynamic buckling under axial step loading of specific imperfect isotropic and anisotropic shells are simulated using this approach. Characteristic results are discussed. The softening behaviour of shells under parametric excitation and the decrease of the buckling load under step loading, as compared with the static case, are illustrated.

Key words: cylindrical shell, dynamic buckling, dynamic stability, parametric excitation

1. Introduction

The stability of structures under dynamic loading constitutes an important research area. Parametric excitation and dynamic buckling are two important fields in the dynamic stability of shell structures [1]. Cylindrical shells are important both from a theoretical and from a practical viewpoint. They are widely used in various branches of engineering. In aerospace, cylindrical shells form the primary structure of missiles and launch vehicles. Thin-walled shell structures are prone to buckling instabilities under static and dynamic compressive loading and they may be directly or parametrically excited into resonance at their natural frequencies by dynamic loads.

A relatively well-defined class of dynamic stability problems is often referred to as parametric excitation problems, i.e. the vibration buckling problem under pulsating loading [2, 3]. The essential ideas for shell problems are discussed by Hsu [4]. The parametric excitation of cylindrical shells was studied by Yao, both in a linear and in a nonlinear context [5, 6], and by Vijayaraghavan and Evan-Iwanowski [7]. Nagai and Yamaki [8] included the effect of boundary conditions and the effect of axisymmetric bending vibrations in the fundamental state in their analysis. The use of laminated structures requires an analysis that takes into account the various couplings in the constitutive equations. Studies in this direction have been carried out by Argento [9] and Argento and Scott [10, 11].

Another important class of dynamic stability problems is the dynamic buckling behaviour under step loading or impulsive loading [12, 13]. For imperfection-sensitive structures the dynamic buckling under

step loading is particularly important, since buckling may occur at lower values than the corresponding static load. In the present study, the term 'dynamic buckling' refers to this specific load case. Several criteria that can be used to estimate the critical load in the dynamic buckling case are discussed in [13]. The dynamic buckling of discrete systems was investigated by Kounadis [14]. Important early studies on dynamic buckling of shells were done by Budiansky and Roth [15] and Roth and Klosner [16]. Tamura and Babcock [17] included parametric excitation effects in their study of dynamic buckling of cylindrical shells under axial step loading. Schokker et al. [18] studied dynamic buckling of composite shells under sudden dynamic pressure.

Both classes of dynamic stability problems (nonlinear parametric excitation and dynamic buckling) are strongly related with the nonlinear (i.e. large amplitude) vibration problem of structures. Research in the field of dynamic stability and nonlinear vibrations has been shifting towards using Finite Elements for the spatial discretization in combination with a transient dynamic analysis, e.g. [19–22]. However, it has been recognized that essential information about the nonlinear dynamic behaviour of structures can be obtained by means of analytical–numerical, low-dimensional models, i.e. models with a small number of degrees of freedom. Within this context the parametric excitation and nonlinear vibration problem of cylindrical shells recently has received considerable attention. Popov et al. [23] used continuation techniques in order to trace the branches of periodic solutions under parametric excitation. Gonçalves and Del Prado [24] used numerical integration to study parametric excitation and escape from the prebuckling potential well. The work in the field of analytical–numerical approaches for shells has been extended towards multi-mode analyses by Pellicano et al. [25] and Pellicano and Amabili [26], who also included the effect of companion mode participation in the parametric excitation problem of cylindrical shells. A recent review of research in the field of nonlinear vibrations of cylindrical shells can be found in [27].

The present paper extends earlier work on nonlinear vibrations of shells [28, 29] and focuses on a simple low-dimensional model presented earlier [29] that is believed to capture important characteristics of the nonlinear dynamic behaviour of an anisotropic cylindrical shell. Donnell-type nonlinear shell equations are used. The effect of the anisotropy of the material, three fundamental loads, imperfections and a nonlinear static state is included. In [29] this model was used to study the nonstationary vibrations of cylindrical shells. In the present paper, both the nonlinear parametric excitation and the dynamic buckling under step loading of thin-walled anisotropic cylindrical shells are analysed. The nonlinear dynamic behaviour is simulated using numerical time-integration. In the case of dynamic buckling, following Budiansky and Roth [15], in the present work the critical load is defined as the load level at which a distinct jump in the maximum response occurs when the load is increased.

2. Governing Equations

The cylindrical shell geometry and the applied loading are defined in Figure 1. The geometry of the shell is characterized by the length L, radius R and (reference) thickness h. The strain energy expression for a cylindrical shell is given by

$$V_0 = \frac{1}{2}\int_0^{2\pi R}\int_0^{L}\left\{N_x\epsilon_x + N_y\epsilon_y + N_{xy}\gamma_{xy} + M_x\kappa_x + M_y\kappa_y + \frac{M_{xy}+M_{yx}}{2}\kappa_{xy}\right\}dx\,dy \tag{1}$$

where $N_x, N_y, \ldots, M_{yx}$ are the usual stress and moment resultants, and $\epsilon_x, \epsilon_y, \ldots, \kappa_{xy}$ the usual strains and curvatures (see e.g. [30]). Using Donnell-type strain–displacement relations and the constitutive

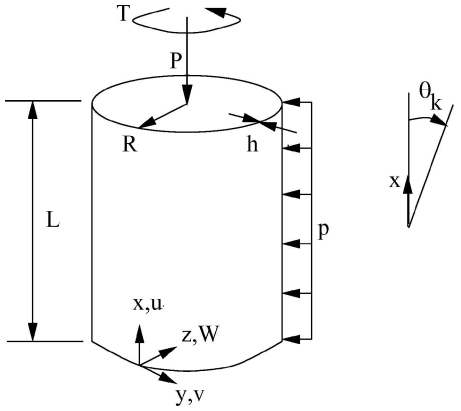

Figure 1. Shell geometry, coordinate system and applied loading.

equations for a general anisotropic shell, the equations governing the nonlinear dynamic behaviour can be derived. The constitutive equations for a laminated shell can be written as

$$\begin{bmatrix} N_x \\ N_y \\ N_{xy} \end{bmatrix} = \begin{bmatrix} A_{11} & A_{12} & A_{16} \\ A_{12} & A_{22} & A_{26} \\ A_{16} & A_{26} & A_{66} \end{bmatrix} \begin{bmatrix} \epsilon_x \\ \epsilon_y \\ \gamma_{xy} \end{bmatrix} + \begin{bmatrix} B_{11} & B_{12} & B_{16} \\ B_{12} & B_{22} & B_{26} \\ B_{16} & B_{26} & B_{66} \end{bmatrix} \begin{bmatrix} \kappa_x \\ \kappa_y \\ \kappa_{xy} \end{bmatrix} \tag{2}$$

$$\begin{bmatrix} M_x \\ M_y \\ \frac{M_{xy}+M_{yx}}{2} \end{bmatrix} = \begin{bmatrix} B_{11} & B_{12} & B_{16} \\ B_{12} & B_{22} & B_{26} \\ B_{16} & B_{26} & B_{66} \end{bmatrix} \begin{bmatrix} \epsilon_x \\ \epsilon_y \\ \gamma_{xy} \end{bmatrix} + \begin{bmatrix} D_{11} & D_{12} & D_{16} \\ D_{12} & D_{22} & D_{26} \\ D_{16} & D_{26} & D_{66} \end{bmatrix} \begin{bmatrix} \kappa_x \\ \kappa_y \\ \kappa_{xy} \end{bmatrix} \tag{3}$$

where the stiffness coefficients A_{ij}, B_{ij} and D_{ij} $(i, j = 1, 2, 6)$ from classical lamination theory are used. The definition of the layer orientation θ_k can be found in Figure 1. The constitutive equations, Equations (2) and (3), can be written in matrix form as

$$\{N\} = A\{\epsilon\} + B\{\kappa\} \tag{4}$$

$$\{M\} = B\{\epsilon\} + D\{\kappa\} \tag{5}$$

and after partial inversion as

$$\{\epsilon\} = A^*\{N\} + B^*\{\kappa\} \tag{6}$$

$$\{M\} = C^*\{N\} + D^*\{\kappa\} \tag{7}$$

where

$$A^* = A^{-1}$$

$$B^* = -A^{-1}B$$

$$C^* = BA^{-1} = -B^{*\mathrm{T}}$$

$$D^* = D - BA^{-1}B$$

Assuming that the radial displacement W is positive inward (see Figure 1) and introducing an Airy stress function F as $N_x = F,_{yy}$, $N_y = F,_{xx}$ and $N_{xy} = -F,_{xy}$, then the Donnell-type nonlinear imperfect shell equations for a general anisotropic material can be written as

$$L_{A^*}(F) - L_{B^*}(W) = -\frac{1}{R}W,_{xx} - \frac{1}{2}L_{\mathrm{NL}}(W, W + 2\bar{W}) \tag{8}$$

$$L_{B^*}(F) + L_{D^*}(W) = \frac{1}{R}F,_{xx} + L_{\mathrm{NL}}(F, W + \bar{W}) + p - \bar{\rho}hW,_{tt} \tag{9}$$

where the variables W and F depend on the time t, $\bar{\rho}hW,_{tt}$ is the radial inertia term, $\bar{\rho}$ the (averaged) specific mass of the laminate, and p the (effective) radial pressure (positive inward). In the following, the partial differential equations will be reduced to a system with a finite number of degrees of freedom. Damping will be introduced in that stage via viscous modal damping terms in the equations of motion of the discretized system. It should be noted that in-plane inertia of the (predominantly) radial modes is neglected in the analysis. However, in the analysis presented in the next section the in-plane inertia of both the fundamental axial and the fundamental torsional mode will be taken into account. The fourth-order linear differential operators

$$L_{A^*}() = A^*_{22}(),_{xxxx} - 2A^*_{26}(),_{xxxy} + (2A^*_{12} + A^*_{66})(),_{xxyy} - 2A^*_{16}(),_{xyyy} + A^*_{11}(),_{yyyy} \tag{10}$$

$$L_{B^*}() = B^*_{21}(),_{xxxx} + (2B^*_{26} - B^*_{61})(),_{xxxy} + (B^*_{11} + B^*_{22} - 2B^*_{66})(),_{xxyy} + (2B^*_{16} - B^*_{62})(),_{xyyy} + B^*_{12}(),_{yyyy} \tag{11}$$

$$L_{D^*}() = D^*_{11}(),_{xxxx} + 4D^*_{16}(),_{xxxy} + 2(D^*_{12} + 2D^*_{66})(),_{xxyy} + 4D^*_{26}(),_{xyyy} + D^*_{22}(),_{yyyy} \tag{12}$$

depend on the stiffness properties of the laminate, and the nonlinear operator defined by

$$L_{\mathrm{NL}}(S, T) = S,_{xx}\, T,_{yy} - 2S,_{xy}\, T,_{xy} + S,_{yy}\, T,_{xx} \tag{13}$$

reflects the geometric nonlinearity. Equation (8) guarantees the compatibility of the strains and the radial displacement field. Equation (9) is the equation of motion in the radial direction.

The shell can be loaded by axial compression P, radial pressure p and counter-clockwise torsion T (Figure 1), both statically ($\tilde{P}$, $\tilde{p}$, $\tilde{T}$) and dynamically ($\hat{P}$, $\hat{p}$, $\hat{T}$). The equations governing the nonlinear dynamic behaviour of a cylindrical shell vibrating about a nonlinear static state will be derived, by expressing both the displacement W and the stress function F as a superposition of two states,

$$W = \tilde{W} + \hat{W} \tag{14}$$

$$F = \tilde{F} + \hat{F} \tag{15}$$

where $\tilde{F}$ and $\tilde{W}$ are the stress function and radial displacement of the static, geometrically nonlinear state which develops under the application of a static load on the imperfect shell, while $\hat{F}$ and $\hat{W}$ are the stress function and radial displacement of the dynamic state corresponding to the large amplitude vibration about the static state. Substituting Equations (14) and (15) into the governing equations, Equations (8) and (9), and regrouping gives sets of equations both for the nonlinear static state and for the nonlinear dynamic state. The Donnell-type equations governing the nonlinear static state of an imperfect anisotropic cylindrical shell become

$$L_{A^*}(\tilde{F}) - L_{B^*}(\tilde{W}) = -\frac{1}{R}\tilde{W},_{xx} - \frac{1}{2}L_{\mathrm{NL}}(\tilde{W}, \tilde{W} + 2\bar{W}) \tag{16}$$

$$L_{B^*}(\tilde{F}) + L_{D^*}(\tilde{W}) = \frac{1}{R}\tilde{F},_{xx} + L_{\mathrm{NL}}(\tilde{F}, \tilde{W} + \bar{W}) + \tilde{p} \tag{17}$$

where $\tilde{p}$ is the static radial loading, and the equations governing the nonlinear dynamic state can be written as

$$L_{A^*}(\hat{F}) - L_{B^*}(\hat{W}) = -\frac{1}{R}\hat{W}_{,xx} - \frac{1}{2}L_{\mathrm{NL}}(\tilde{W}, \hat{W}) - \frac{1}{2}L_{\mathrm{NL}}(\hat{W}, \tilde{W} + 2\bar{W}) - \frac{1}{2}L_{\mathrm{NL}}(\hat{W}, \hat{W}) \tag{18}$$

$$L_{B^*}(\hat{F}) + L_{D^*}(\hat{W}) = \frac{1}{R}\hat{F}_{,xx} + L_{\mathrm{NL}}(\tilde{F}, \hat{W}) + L_{\mathrm{NL}}(\hat{F}, \tilde{W} + \bar{W}) + L_{\mathrm{NL}}(\hat{F}, \hat{W}) - \bar{\rho}h\hat{W}_{,tt} + \hat{p} \tag{19}$$

where $\hat{p}$ is the dynamic radial loading.

3. Analysis

Approximate solutions for the equations governing the nonlinear static state are obtained via a Galerkin procedure using a limited number of assumed deflection modes. A two-mode imperfection model, consisting of an axisymmetric and an asymmetric mode, is used. The static-state response is assumed to be affine to the given imperfection. In the case that the imperfection and response mode correspond to the lowest buckling mode, this model is expected to capture important characteristics of the static behaviour. A set of three nonlinear equations is obtained that can be solved for the unknown displacement amplitudes. Details of this method can be found in [31].

To find approximate solutions for the equations governing the dynamic state, based on a small number of assumed deflection modes, the energy expressions corresponding to the governing differential equations are used as a starting point for the dynamic analysis [31]. Using the splitting of variables given in Equations (14) and (15) one obtains the energy expressions for both the static state (corresponding to Equations (16) and (17)) and the dynamic state (corresponding to Equations (18) and (19)). Hamilton's (extended) variational principle corresponding to Equations (18) and (19) can be stated as

$$\int_{t_1}^{t_2} \delta(T - \hat{V})dt + \int_{t_1}^{t_2} \delta(W_{\mathrm{nc}})dt = 0 \tag{20}$$

where T is the total kinetic energy, $\hat{V}$ the potential energy of the dynamic state, and W_{nc} the work done by nonconservative forces. It should be noted that the coefficients of the dynamic-state problem depend on the solution of the static-state problem, Equations (16) and (17).

For the dynamic state, the radial pressure is split into a conservative part and a nonconservative part. The in-plane loads (axial compressive load and counter-clockwise torque) are applied at $x = L$ and correspond to averaged stress resultants. They are also split into a conservative part and a nonconservative part:

$$\hat{p} = \hat{p}^{\mathrm{c}} + \hat{p}^{\mathrm{nc}}; \quad \hat{N}_x|_{x=L} = \hat{N}_x^{\mathrm{c}} + \hat{N}_x^{\mathrm{nc}}; \quad \hat{N}_{xy}|_{x=L} = \hat{N}_{xy}^{\mathrm{c}} + \hat{N}_{xy}^{\mathrm{nc}} \tag{21}$$

where the superscript c denotes the conservative part, and superscript nc the nonconservative part. The conservative parts of the loading correspond to an applied step loading. At $x = 0$ the in-plane displacements u and v (averaged in the circumferential direction) are assumed to be zero.

The potential energy for the dynamic state then becomes

$$\hat{V} = \hat{V}_0 + \hat{V}_1 \tag{22}$$

where $\hat{V}_0$ is the strain energy and $\hat{V}_1$ the potential energy of the applied conservative loads. The potential energy of the applied conservative loads can be written as

$$\hat{V}_1 = -\int_0^{2\pi R} \hat{N}_x^{\mathrm{c}} \int_0^L \hat{u}_{,x}\, dx\, dy - \int_0^{2\pi R} \int_0^L \hat{p}^{\mathrm{c}} \hat{W}\, dx\, dy - \int_0^{2\pi R} \hat{N}_{xy}^{\mathrm{c}} \int_0^L \hat{v}_{,x}\, dx\, dy \tag{23}$$

where $\hat{N}_x^{\mathrm{c}} = -\hat{N}_0 u_{\mathrm{H}}(t)$ is the applied axial step load, $\hat{p}^{\mathrm{c}} = \hat{p}_0 u_{\mathrm{H}}(t)$ the applied external pressure step load, and $\hat{N}_x^{\mathrm{c}} = \hat{T}_0 u_{\mathrm{H}}(t)$ the applied counter-clockwise torsional step load. Here, $u_{\mathrm{H}}(t)$ denotes the Heaviside unit step function.

The virtual work done by the nonconservative forces is

$$\delta W_{\mathrm{nc}} = \int_0^{2\pi R} \hat{N}_x^{\mathrm{nc}} \int_0^L \delta\hat{u}_{,x}\, dx\, dy + \int_0^{2\pi R} \int_0^L \hat{p}^{\mathrm{nc}} \delta\hat{W}\, dx\, dy + \int_0^{2\pi R} \hat{N}_{xy}^{\mathrm{nc}} \int_0^L \delta\hat{v}_{,x}\, dx\, dy \tag{24}$$

where $\hat{N}_x^{\mathrm{nc}}$, $\hat{p}^{\mathrm{nc}}$ and $\hat{N}_{xy}^{\mathrm{nc}}$ are the axial, radial, and torsional nonconservative load, respectively.

The kinetic energy of the shell is given by

$$T_{\mathrm{s}} = T_{\mathrm{o}} + T_{\mathrm{i}} \tag{25}$$

where the out-of-plane inertia contribution T_{o} is given by

$$T_{\mathrm{o}} = \frac{1}{2}\bar{\rho} h \int_0^{2\pi R} \int_0^L \left(\frac{\partial \hat{W}}{\partial t}\right)^2 dx\, dy \tag{26}$$

and the in-plane inertia contribution T_{i} is given by

$$T_{\mathrm{i}} = \frac{1}{2}\bar{\rho} h \int_0^{2\pi R} \int_0^L \left\{ \left(\frac{\partial \hat{u}}{\partial t}\right)^2 + \left(\frac{\partial \hat{v}}{\partial t}\right)^2 \right\} dx\, dy \tag{27}$$

For a discretized system with N generalized coordinates (degrees of freedom) q_i, application of Hamilton's principle leads to the Lagrange's equations of motion:

$$\frac{d}{dt}\left(\frac{\partial T}{\partial \dot{q}_i}\right) - \frac{\partial T}{\partial q_i} + \frac{\partial V}{\partial q_i} = Q_i, \quad i = 1, 2, \ldots, N \tag{28}$$

where the generalized forces Q_i, corresponding to the generalized coordinates q_i, are defined by $\delta W_{\mathrm{nc}} = \sum_i Q_i \delta q_i$.

Assuming a radial displacement $\hat{W} = \hat{W}(\xi_i)$, depending on the generalized coordinates ξ_i ($i = 1, 2, \ldots, N-2$), a particular solution for the stress function $\hat{F}_{\mathrm{p}} = \hat{F}_{\mathrm{p}}(\xi_i)$ can be obtained directly from the dynamic-state compatibility equation, Equation (18) [31]. The solution for $\hat{F}$ becomes

$$\hat{F} = \hat{F}_{\mathrm{p}} + \hat{F}^* \tag{29}$$

where the complementary solution $\hat{F}^*$, corresponding to stress resultants which are constant over the shell, can be written as

$$\hat{F}^* = \frac{1}{2}\hat{N}_x^* y^2 + \frac{1}{2}\hat{N}_y^* x^2 - \hat{N}_{xy}^* xy \tag{30}$$

while the corresponding complementary in-plane displacements $\hat{u}^*$ and $\hat{v}^*$ are assumed, for a fixed end at $x = 0$, as

$$\hat{u}^* = -\left(\frac{C_a h}{L}\right) x; \quad \hat{v}^* = -\left(\frac{C_t h}{L}\right) x \tag{31}$$

The two additional generalized coordinates C_a and C_t introduced here can be related to the spatially constant stress resultants $\hat{N}_x^*$, $\hat{N}_y^*$ and $\hat{N}_{xy}^*$, and to the generalized coordinates ξ_i via the boundary conditions for averaged in-plane stress resultants and via the circumferential periodicity condition:

$$\int_0^{2\pi R} \int_0^L \hat{u}_{,x}\, dx\, dy = -2\pi RhC_a = f_{1,\text{lin}}(\hat{N}_x^*, \hat{N}_y^*, \hat{N}_{xy}^*) + f_{1,\text{nl}}(\xi_i) \tag{32}$$

$$\int_0^{2\pi R} \hat{v}_{,y}\, dy = 0 = f_{2,\text{lin}}(\hat{N}_x^*, \hat{N}_y^*, \hat{N}_{xy}^*) + f_{2,\text{nl}}(\xi_i) \tag{33}$$

$$\int_0^{2\pi R} \int_0^L \hat{v}_{,x}\, dx\, dy = -2\pi RhC_t = f_{3,\text{lin}}(\hat{N}_x^*, \hat{N}_y^*, \hat{N}_{xy}^*) + f_{3,\text{nl}}(\xi_i) \tag{34}$$

where $f_{j,\text{lin}}$ ($j = 1, 2, 3$) are linear functions of the constant stresses, and $f_{j,\text{nl}}$ are nonlinear functions of the generalized coordinates ξ_i ($i = 1, 2, \ldots, N-2$). The functions are obtained by using the strain–displacement relations in combination with the partially inverted constitutive equations, Equation (7).

Inverting the relations in Equations (32)–(34) we can obtain the unknown (spatially) constant stress resultants as functions of C_a, C_t and ξ_i,

$$\hat{N}_x^* = g_1(C_a, C_t, \xi_i); \quad \hat{N}_y^* = g_2(C_a, C_t, \xi_i); \quad \hat{N}_{xy}^* = g_3(C_a, C_t, \xi_i) \tag{35}$$

These expressions can be found in [31]. In the present approach, the averaged stress resultants are prescribed.

The shell inertia forces are obtained from the kinetic energy expressions for T_o and T_i, Equations (26) and (27). The in-plane inertia of the radial modes is neglected, but the in-plane inertia of both the fundamental axial and the fundamental torsional mode will be taken into account approximately by including the complementary in-plane displacements $u = \hat{u}^*$ and $v = \hat{v}^*$ in T_i. The kinetic energy due to a ring or disk at the loaded end of the shell is given by

$$T_\text{m} = \frac{1}{2} m \left(\frac{\partial \hat{u}^*}{\partial t}\right)^2 \Bigg|_{x=L} + \frac{1}{2} \frac{I_\text{p}}{R^2} \left(\frac{\partial \hat{v}^*}{\partial t}\right)^2 \Bigg|_{x=L} = \frac{1}{2} m (C_a h)^2 + \frac{1}{2} I_\text{p} (C_t \frac{h}{R})^2 \tag{36}$$

where m is the mass and I_p the polar moment of inertia of the ring or disk. The total kinetic energy of the system is then given by

$$T = T_\text{s} + T_\text{m} \tag{37}$$

Substitution of the given imperfection mode $\bar{W}$, the assumed radial deflections of the static state $\tilde{W}$ and dynamic state $\hat{W}$, and the particular solutions for the stress functions $\tilde{F}$ and $\hat{F}$ into the energy expression, leads to a coupled set of nonlinear ordinary differential equations in the unknown time-dependent generalized coordinates C_a, C_t, ξ_i ($i = 1, 2, \ldots, N-2$), or q_i ($i = 1, 2, \ldots, N$). For

normal coordinates the equations can be written in the following form:

$$\ddot{q}_i + k_i q_i + \sum_{j=1}^{N}\sum_{k=1}^{N} a_{ijk} q_j q_k + \sum_{j=1}^{N}\sum_{k=1}^{N}\sum_{l=1}^{N} b_{ijkl} q_j q_k q_l = g_i \tag{38}$$

where k_i, a_{ijk} and b_{ijkl} are coefficients which can in general depend on time, and g_i is the forcing term. The coefficients can be found in [31]. Modal viscous damping is introduced in the analysis by adding terms of the form $c_i \dot{q}_i$ ($\zeta_i = \frac{c_i}{2\sqrt{k_i}}$) in Equation (38).

4. Application to Parametric Excitation and Dynamic Buckling

The procedure described in the previous section can be applied to nonlinear flexural vibrations [29], to dynamic buckling (buckling under step loading), and to parametric excitation (vibration buckling under pulsating loads) of anisotropic cylindrical shells. In the present paper, results for parametric excitation and dynamic buckling of specific isotropic and anisotropic shells will be presented. The essential axisymmetric modes and the companion mode are included in the formulation. Further, the effect of the inertia of the fundamental axial and torsional mode is taken into account.

In order to investigate the nonlinear dynamic behaviour of statically loaded imperfect anisotropic cylindrical shells, for the imperfection and static response the following deflection functions are used:

Imperfection:

$$\bar{W}/h = \bar{\xi}_1 \cos\frac{2m\pi x}{L} + \bar{\xi}_2 \sin\frac{m\pi x}{L} \cos\frac{n}{R}(y - \tau_K x) \tag{39}$$

Static state:

$$\tilde{W}/h = \tilde{\xi}_0 + \tilde{\xi}_1 \cos\frac{2m\pi x}{L} + \tilde{\xi}_2 \sin\frac{m\pi x}{L} \cos\frac{n}{R}(y - \tau_K x) \tag{40}$$

where m denotes the number of half waves in axial direction, n is the number of full waves in the circumferential direction of the imperfection and static response mode, and τ_K is Khot's skewedness parameter [32], introduced to account for the skewedness of the asymmetric modes which appears under torsional loading and which may occur due to torsion-bending coupling in the constitutive equations. Further, $\bar{\xi}_1$ and $\bar{\xi}_2$ are the imperfection amplitudes and $\tilde{\xi}_0$, $\tilde{\xi}_1$, and $\tilde{\xi}_2$ are the static response amplitudes.

The following displacement is assumed for the *dynamic state*:

$$\begin{aligned}\hat{W}/h = {} & C_0(t) + C_1(t)\cos\frac{2m\pi x}{L} + A(t)\sin\frac{m\pi x}{L}\cos\frac{\ell}{R}(y - \tau_K x) \\ & + B(t)\sin\frac{m\pi x}{L}\sin\frac{\ell}{R}(y - \tau_K x)\end{aligned} \tag{41}$$

where ℓ is the number of full waves in the circumferential direction of the dynamic response mode, and where the generalized coordinates ξ_i, in this case A, B, C_0 and C_1, depend on time.

The effect of the inertia of the fundamental in-plane (axial and torsional) modes is taken into account via the approach discussed in Section 3. In this method, introduced in [17], the complementary in-plane displacements, Equation (31), are included in the formulation,

$$\hat{u}^* = -\left(\frac{C_a h}{L}\right) x; \quad \hat{v}^* = -\left(\frac{C_t h}{L}\right) x$$

In this case, the kinetic energy in Equation (37) is the sum of the kinetic energy of the shell, Equation (25), and the kinetic energy of the end ring, Equation (36).

4.1. Nonlinear Parametric Excitation

The imperfection and static response modes, Equations (39) and (40), are used to describe the behaviour of the anisotropic cylindrical shell under a static loading consisting of the three basic axisymmetric loads. In addition, the shell is loaded by the parametric axial, torsional, and radial loading given by

$$\hat{N}_x^{\mathrm{nc}} = -\hat{N}_0 \cos \Omega_{\mathrm{e}} t; \quad \hat{N}_{xy}^{\mathrm{nc}} = \hat{T}_0 \cos \Omega_{\mathrm{e}} t; \quad \hat{p}^{\mathrm{nc}} = \hat{p}_0 \cos \Omega_{\mathrm{e}} t \tag{42}$$

where $\hat{N}_0$, $\hat{T}_0$ and $\hat{p}_0$ are constants, and where Ω_{e} is the frequency of the applied load. The radial response under parametric excitation is described by the displacement function in Equation (41).

4.2. Dynamic Buckling

In order to model the dynamic buckling behaviour under step loading, the displacement functions for the two-mode imperfection, Equation (39), and corresponding static response, Equation (40), are again used. In the special case of dynamic buckling under step loading, the applied loads become

$$\hat{N}_x^{\mathrm{c}} = -\hat{N}_0 u_{\mathrm{H}}(t); \quad \hat{N}_{xy}^{\mathrm{c}} = \hat{T}_0 u_{\mathrm{H}}(t); \quad \hat{p}^{\mathrm{c}} = \hat{p}_0 u_{\mathrm{H}}(t) \tag{43}$$

where $u_{\mathrm{H}}(t)$ is the unit step function, $\hat{N}_0$, $\hat{T}_0$ and $\hat{p}_0$ denote the (constant) amplitudes. It is assumed that the radial displacement of the dynamic state can be described by the deflection function in Equation (41).

5. Results and Discussion

The detailed derivations of the analysis described in the previous section have been carried out using the symbolic manipulation program REDUCE [33] and can be found in [31]. The results were coded in a FORTRAN computer program. The Adams–Moulton method with adaptive step size is used for the numerical integration of the ordinary differential equations. In principle, general loading conditions (axial compression, radial pressure and torsion) can be considered. In this paper, characteristic results will be shown for specific isotropic and anisotropic shells under axial parametric excitation, and for the dynamic buckling behaviour under axial step loading. The data of the shells that have been used in the calculations are as follows (E is Young's modulus, G is the shear modulus, and ν is Poisson's ratio).

Booton's shell: An anisotropic shell used earlier in static stability investigations [34]. The data are given in Table 1. For this anisotropic shell, $E = E_{11}$ and $\nu = \nu_{12}$ will be used as reference values.

Bogdanovich' shell: Isotropic shell [35]: $R = 1$ m, $R/h = 100$, $L/R = 2$, $E = 4 \times 10^{10}$ N/m^2, $\nu = 0.3$, $\bar{\rho} = 2.5 \times 10^3$ kg/m^3.

Popov's shell: Isotropic shell [23]: $R = 0.2$ m, $h = 0.002$ m, $L = 0.4$ m, $E = 2.1 \times 10^{11}$ N/m^2, $\nu = 0.3$, $\bar{\rho} = 7.85 \times 10^3$ kg/m^3.

Tamura's shell: Isotropic shell [17]: $R = 101.6$ mm, $h = 0.1016$ mm, $L = 203.2$ mm, $\nu = 0.3$.

Table 1. Booton's anisotropic shell.

Shell geometry	$R = 67.8$ mm
	$L = 135.6$ mm
Laminate geometry	Three layers
	(numbering from outside)
	$h_1 = h_2 = h_3 = 0.226$ mm
	$\theta_1 = 30^\circ, \theta_2 = 0^\circ, \theta_3 = -30^\circ$
	(Figure 1)
Layer properties	Glass-epoxy
	$E_{11} = 4.02 \times 10^4$ MPa
	$E_{22} = 1.67 \times 10^4$ MPa
	$\nu_{12} = 0.363$
	$G_{12} = 4.61 \times 10^3$ MPa

5.1. Parametric Excitation

The first example for parametric excitation concerns the type of nonlinearity for moderately large amplitudes. To analyse the 'single' mode vibrations, i.e. assuming a single primary mode, it is necessary to include axisymmetric modes in the assumed response [23, 24, 26]. The shell is subjected to a parametric axial loading,

$$\hat{N}_x^{\mathrm{nc}} = -\hat{N}_0 \cos \Omega_e t; \quad \hat{N}_{xy}^{\mathrm{nc}} = 0; \quad \hat{p}^{\mathrm{nc}} = 0$$

The amplitude of the excitation is $\hat{\lambda} = \hat{N}_0/N_{\mathrm{cl}} = 0.35$, where $N_{\mathrm{cl}} = (Eh^2)/(cR)$, $N_0 = -N_x(x = L)$, and $c = \sqrt{3(1-\nu^2)}$. In addition, the shell is subjected to static axial pre-vibration loading $\tilde{\lambda} = \tilde{N}_0/N_{\mathrm{cl}}$. The shell has an asymmetric imperfection

$$\bar{W}/h = 0.01 \sin \frac{\pi x}{L} \cos \frac{5}{R} y$$

It is noted that for this imperfect shell, the applied axial load will induce the static deformations

$$\tilde{W}/h = \tilde{\xi}_0 + \tilde{\xi}_1 \cos \frac{2\pi x}{L} + \tilde{\xi}_2 \sin \frac{\pi x}{L} \cos \frac{5}{R} y \tag{44}$$

and the corresponding stresses.

The dynamic response mode is assumed to be

$$\hat{W}/h = C_0(t) + C_1(t) \cos \frac{2\pi x}{L} + A(t) \sin \frac{\pi x}{L} \cos \frac{5}{R} y \tag{45}$$

which, in addition to the asymmetric mode, includes the corresponding axisymmetric modes. For the 'single' mode vibration of this isotropic shell vibrating with $m = 1$ and $\ell = 5$, in [35] a hardening behaviour is obtained, whereas the present model predicts a softening behaviour. This is illustrated in Figure 2, which shows the response of Bogdanovich' shell under parametric axial loading.

Frequency–response curves have been obtained via numerical time-integration. Damping was neglected (damping parameter $\zeta_A = \frac{c_A}{2\sqrt{k_A}} = 0$). The response amplitude increases in time, and after a

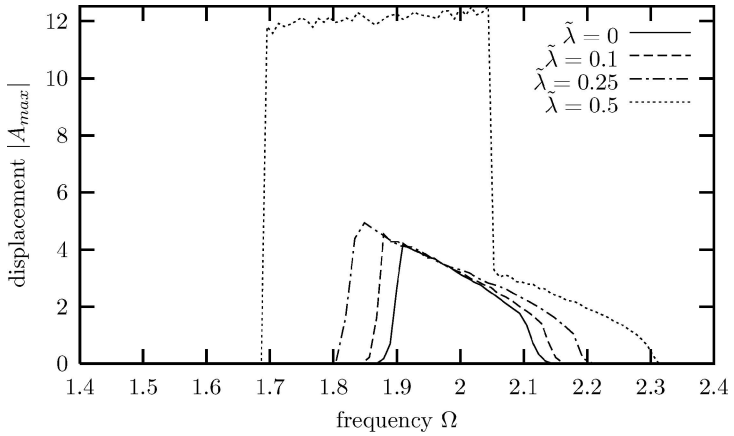

Figure 2. Frequency-response curves for 'single' mode vibration under parametric excitation and different static axial loads $\tilde{\lambda}$ for Bogdanovich' isotropic shell. Forcing frequency $\Omega = \Omega_e/\omega_{lin}$.

rapid build-up has occurred it reaches a maximum. An integration time of 50 forcing periods $T = 2\pi/\Omega_e$ was sufficient to capture this maximum. The maximum response during the integration interval has been plotted as a function of the forcing frequency in Figure 2. The forcing frequency is normalized with respect to ω_{lin}, the linear frequency of the statically loaded imperfect shell (for $\tilde{\lambda} = 0.5$, $\omega_{lin} = 346.92$ rad/s, for $\tilde{\lambda} = 0.25$, $\omega_{lin} = 424.26$ rad/s, for $\tilde{\lambda} = 0.1$, $\omega_{lin} = 464.56$ rad/s, and for $\tilde{\lambda} = 0$, $\omega_{lin} = 489.59$ rad/s).

It is well known that for perfect shells [4] for certain values of the frequency of the applied load, a Mathieu-type instability occurs. The trivial axisymmetric solution with period T becomes unstable and a period-doubling bifurcation occurs. Periodic vibrations in an, initially quiescent, asymmetric mode are possible with period $2T$. In the case of an unloaded or loaded shell with asymmetric imperfection, the parametrically excited asymmetric mode will already respond from the outset.

Varying the excitation frequency, response curves are obtained that are typical of a softening behaviour. The response curves 'bend backwards', resulting in upward jumps for the upward frequency sweep and downward jumps for the downward sweep. At the static axial load level $\tilde{\lambda} = 0.5$, the response jumps to a remote static response branch. Both the softening behaviour observed and the escape from the prebuckling state potential well [24] are captured by the present model because of the inclusion of axisymmetric modes in the assumed deflection function, Equation (45). If the axisymmetric modes are not included, one misses these phenomena [23, 24].

The second case that will be discussed deals with the parametric excitation problem of an isotropic perfect shell, earlier studied by other investigators [23, 24, 26]. Continuation techniques have been used in [23] and [26] in order to trace the branches of periodic solutions. This approach is efficient in particular in the case of zero or low damping. To obtain the nonstationary responses one has to resort to numerical integration.

In the present study the response was obtained using numerical integration. Load increments in $\hat{\lambda} = \hat{N}_0/N_{cl}$ of 0.001 were used, and numerical integration over 1000 forcing periods was performed for each load level. The end conditions at each load level were used as initial conditions for the next level. The critical dynamic loads under parametric excitation are given in Table 2 where they are compared with results from Pellicano and Amabili [26]. In the present case the critical load is defined as the load at which for small perturbations in the asymmetric mode, a growing solution of the asymmetric mode, or a jump of the asymmetric mode to a remote branch, occurs. Results including the effect of in-plane

Table 2. Critical dynamic load under parametric excitation.

$\omega/\omega_{1,5}$	ζ_i	$\hat{N}_0/N_{\text{cl}}$		
		Equation (41)	Equations (41) and (31)	[26]
1.9	0.089	0.473	0.439	0.448
2.0	0.089	0.434	0.400	0.416
2.1	0.089	0.524	0.479	0.492
1.9	0.016	0.253	0.235	0.24
1.9	0.089 (Kelvin–Voight)	0.484	0.449	0.46

Popov's shell. Kelvin–Voight: $\zeta_A = \zeta_B = 0.089$, $\zeta = 0.001$ for all other modes. In other cases ζ_i has the same value for all modes.

inertia are also included in the table. A small amount of damping ($\zeta = 0.001$) was added for the other modes in the Kelvin–Voight case.

As in [26], the axisymmetric response follows from a dynamic analysis, but the 'simply supported' boundary conditions are not taken into account rigorously in the present approach. The present critical loads are 5–7% higher than the results from the more extensive model used in [26] (Table 2). Pellicano et al. [25] presented a careful study of the convergence characteristics of their modal expansion method in the case of nonlinear vibrations. The results of the present analysis including the effect of in-plane inertia of the in-plane modes, Equations (31), show a moderate decrease as compared with the case in which in-plane inertia is not taken into account.

In [26] companion mode response was observed. The companion mode, the 'B-mode' in Equation (41), is also included in the present formulation, and is given a small disturbance in the numerical simulations. In the present work companion mode participation is defined as the situation in which the 'B-mode' is parametrically excited due to the (nonlinear) contribution of the axisymmetric modes. In the cases investigated companion mode participation in this sense, where the 'B-mode' and the 'A-mode' are (approximately) 90° out-of-phase, has not been found.

A characteristic result for the parametric vibrations of Booton's anisotropic shell is depicted in Figure 3. The figure shows the frequency–response curve of the vibration mode

$$\hat{W}(t)/h = C_0(t) + C_1(t)\cos\frac{2\pi x}{L} + A(t)\sin\frac{\pi x}{L}\cos\frac{6}{R}(y - \tau_K x)$$

with $\tau_K = -0.002$.

The shell is subjected to a pulsating axial load,

$$\hat{N}_x^{\text{nc}} = -\hat{N}_0\cos\Omega_{\text{e}}t; \quad \hat{N}_{xy}^{\text{nc}} = 0; \quad \hat{p}^{\text{nc}} = 0$$

with amplitude $\hat{\lambda} = \hat{N}_0/N_{\text{cl}} = 0.1$. The following two-mode imperfection is assumed:

$$\bar{W}/h = -0.04\cos\frac{2\pi x}{L} + 0.05\sin\frac{\pi x}{L}\cos\frac{6}{R}(y - \tau_K x)$$

with $\tau_K = -0.002$. Damping is neglected ($\zeta_A = \zeta_{C_0} = \zeta_{C_1} = 0$). The effect of the inertia of the fundamental in-plane modes is not taken into account. The maximum response during the integration time of 200 forcing periods T (where $T = 2\pi/\Omega_{\text{e}}$) is plotted as a function of the forcing frequency. The forcing frequency is normalized with respect to ω_{lin}, the linear frequency of the *imperfect* shell.

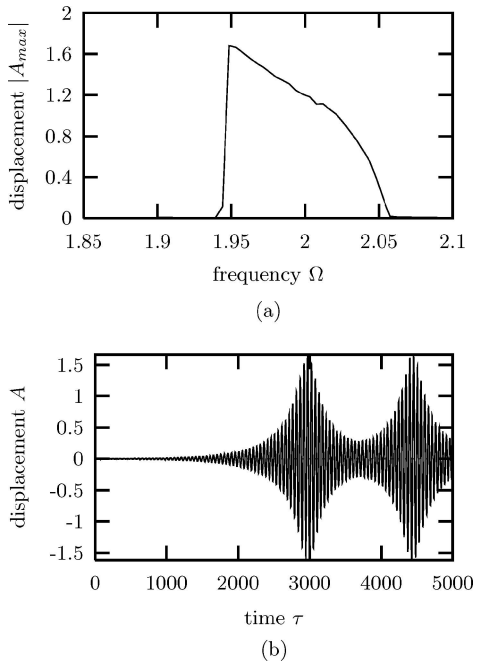

Figure 3. Parametric excitation of Booton's anisotropic shell: (a) frequency–response curve, (b) time history at $\Omega = \Omega_e/\omega_{lin} = 1.95$. Forcing frequency $\Omega = \Omega_e/\omega_{lin}$.

The response in time is shown for a forcing frequency $\Omega = \Omega_e/\omega_{lin} = 1.95$. The initial conditions were $A(t = 0) = \dot{A}(t = 0) = 0$. Initially, the response amplitude remains small for several forcing periods, until between $\tau = (1/R)\sqrt{(E/\bar{\rho})}t = 2000$ and $\tau = 3000$ a rapid build-up occurs. It is noted that if damping is present, depending on the value of the damping parameter, gradually the beating character of the response disappears with time, and the amplitude tends to go to a constant value, cf. [6].

5.2. Dynamic Buckling Under Step Loading

Characteristics of the analysis will first be discussed briefly for Tamura's shell. In Figure 4, results for the dynamic buckling of this shell under axial step loading are depicted,

$$\hat{N}_x^c = -\hat{N}_0 u_H(t); \quad \hat{N}_{xy}^c = 0; \quad \hat{p}^c = 0$$

The inertia of the axial mode

$$\hat{u}^* = -\left(\frac{C_a h}{L}\right) x$$

is included (see Equation (31)). The damping parameter corresponding to the fundamental axial mode $\zeta_{C_a} = 0.2$.

Under axial step loading, the vibration in the axial mode can parametrically induce buckling. In [17] it was shown that bending modes with a high axial wave number can be sensitive to this type of buckling.

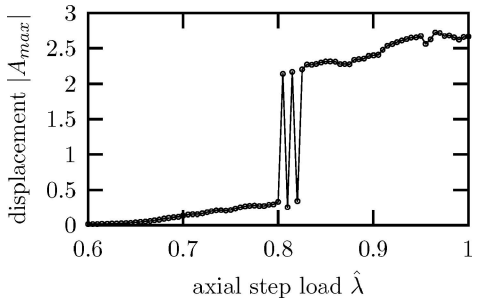

Figure 4. Maximum response under axial step loading for Tamura's isotropic shell.

In the present example, the shell is assumed to buckle in the mode $(m, \ell) = (20, 29)$,

$$\hat{W}(t)/h = C_0(t) + C_1(t)\cos\frac{40\pi x}{L} + A(t)\sin\frac{20\pi x}{L}\cos\frac{29}{R}y \tag{46}$$

For this case dynamic buckling is induced by the parametric axial loading that corresponds to the vibration in the axial mode. The maximum response of the asymmetric mode during an integration time τ_{fin} of 400 ($\tau = (1/R)\sqrt{(E/\bar{\rho})}t$) has been used to plot the load–response curve, which shows a clear jump when the load is increased from $\hat{\lambda} = \hat{N}_0/N_{\text{cl}} = 0.80$ to $\hat{\lambda} = 0.805$. The latter load level can be defined as the dynamic buckling load, corresponding to the well-known Budiansky–Roth criterion [15].

For all load values $\hat{\lambda}$ greater than 0.825, the applied step load will result in an escape to a remote static equilibrium path. Due to interactions of the different modes involved, it is possible that for certain load values between $\hat{\lambda} = 0.805$ and $\hat{\lambda} = 0.825$ the shell buckles dynamically, i.e. the shell escapes from the prebuckling state potential well to the remote branch, while for a slightly different load value the response remains small during the integration time considered. This is illustrated in Figure 4, where for $\hat{\lambda} = 0.810$ and $\hat{\lambda} = 0.820$ the response remains small, while for $\hat{\lambda} = 0.815$ dynamic buckling does occur. This type of behaviour was also found earlier [17]. Another example of this phenomenon will be shown later for Booton's shell (Figure 8). Time histories (to $\tau = (1/R)\sqrt{(E/\bar{\rho})}t = 200$) of the different displacement components for two characteristic values of the loading near the dynamic buckling load are shown in Figure 5.

The second example of dynamic buckling concerns the behaviour of Booton's anisotropic shell under axial step loading. In Figure 6, static response curves of Booton's shell are shown for the mode (3, 5, −1.56),

$$\tilde{W}/h = \tilde{\xi}_0 + \tilde{\xi}_1\cos\frac{6\pi x}{L} + \tilde{\xi}_2\sin\frac{3\pi x}{L}\cos\frac{5}{R}(y - \tau_K x)$$

with $\tau_K = -1.56$, the mode corresponding to the lowest static bifurcation buckling load $\lambda_{m\ell\tau} = 0.407$. The response curve corresponding to the mode with the same m and ℓ but without skewedness, $(m, \ell, \tau_K) = (3, 5, 0)$, is also shown in this figure. The static bifurcation buckling load of this mode occurs at $\lambda = 0.829$. The buckling load of the corresponding axisymmetric mode (2m, 0) = (6, 0) occurs at $\lambda = 0.501$. In both cases, the imperfection amplitudes assumed are $\bar{\xi}_1 = -0.04$ and $\bar{\xi}_2 = 0.05$. Static response curves for the mode corresponding to the lowest vibration frequency, $(m, \ell, \tau_K) = (1, 6, -0.002)$, can be found in Figure 7.

After characterizing the static behaviour of the cases $(m, \ell, \tau_K) = (3, 5, -1.56)$, $(m, \ell, \tau_K) = (3, 5, 0)$, and $(m, \ell, \tau_K) = (1, 6, -0.002)$, results for Booton's anisotropic shell under axial step loading

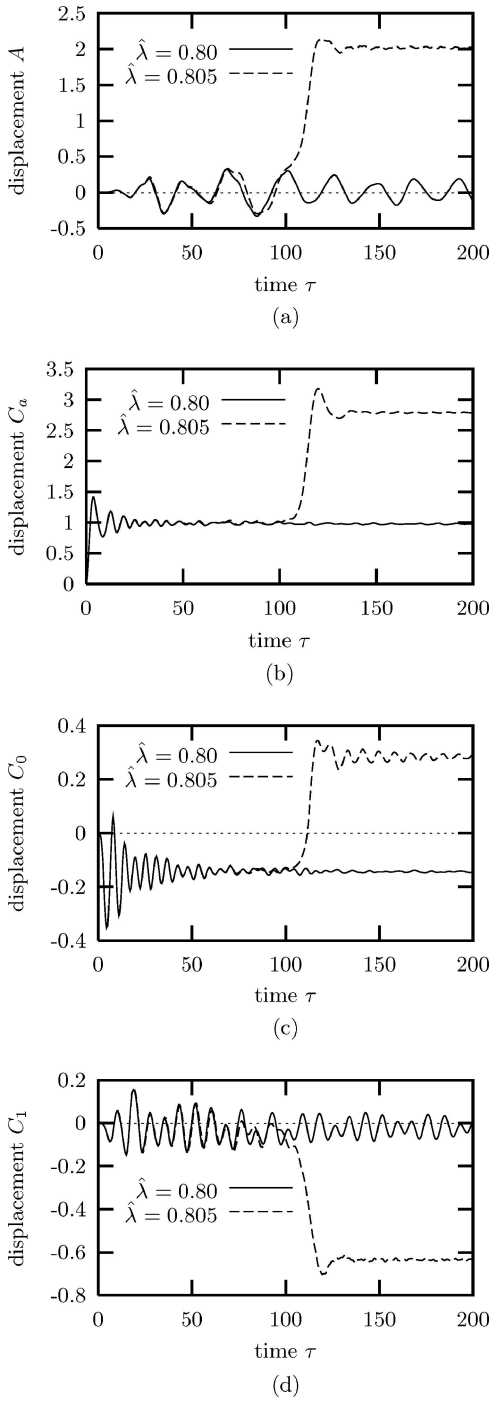

Figure 5. Time histories of the different displacement components near the dynamic buckling load of Tamura's isotropic shell: (a) asymmetric mode, (b) axial mode, (c) constant axisymmetric mode and (d) double harmonic axisymmetric mode.

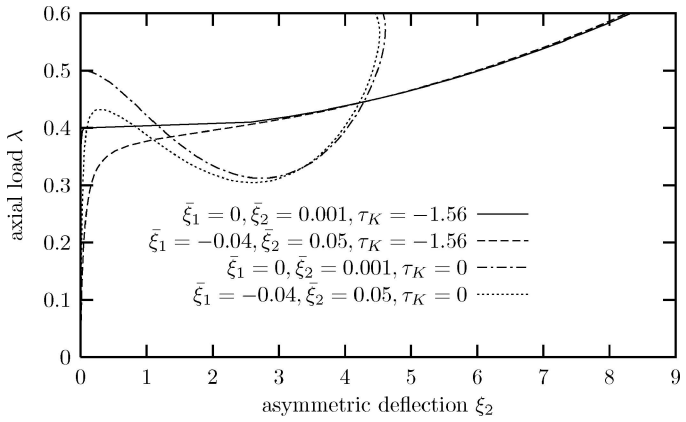

Figure 6. Static asymmetric mode response of imperfect Booton's anisotropic shell: response mode (3,5,τ_K), static buckling modes.

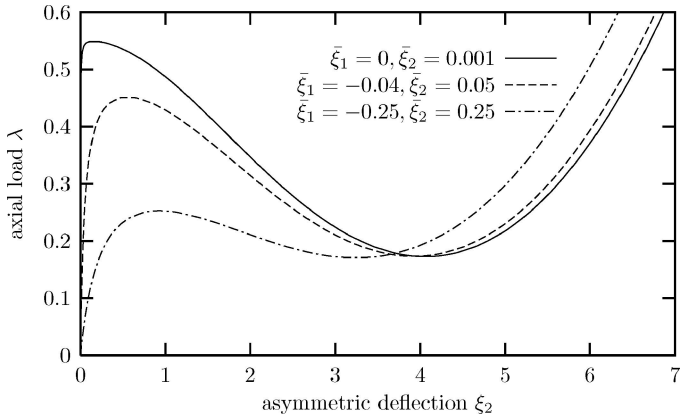

Figure 7. Static asymmetric mode response of imperfect Booton's anisotropic shell: response mode (1,6,−0.002), lowest vibration mode of the unloaded perfect structure.

are depicted in Figure 8. The maximum response of the asymmetric mode during an integration time τ_{fin} of 2000 ($\tau = (1/R)\sqrt{(E/\bar{\rho})}t$) was used to plot the load-response curve.

In Figure 8a, the shell is assumed to buckle dynamically in the mode $(m, \ell, \tau_K) = (3, 5, -1.56)$,

$$\hat{W}(t)/h = C_0(t) + C_1(t)\cos\frac{6\pi x}{L} + A(t)\sin\frac{3\pi x}{L}\cos\frac{5}{R}(y - \tau_K x)$$

with $\tau_K = -1.56$. This mode corresponds to static buckling. The imperfection amplitudes are $\bar{\xi}_1 = -0.04$ and $\bar{\xi}_2 = 0.05$,

$$\bar{W}/h = -0.04\cos\frac{6\pi x}{L} + 0.05\sin\frac{3\pi x}{L}\cos\frac{5}{R}(y - \tau_K x)$$

with $\tau_K = -1.56$. The inertia of the in-plane modes has not been taken into account, and damping is neglected ($\zeta_A = 0$). The maximum response is given as a function of the applied step load. It is noted that a clear jump in this curve does not occur in this case, since the buckling mode considered has a stable static postbuckling behaviour.

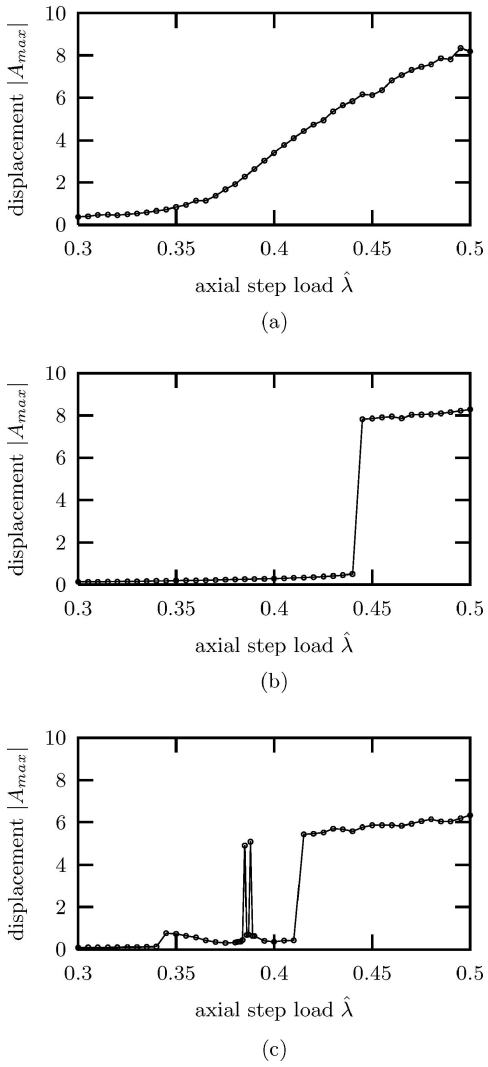

Figure 8. Maximum response under axial step loading of Booton's anisotropic shell: (a) mode (3, 5, −1.56), (b) mode (1, 6, −0.002), (c) mode (3, 5, 0).

The mode corresponding to the lowest vibration mode is imperfection sensitive and the response curve shows a distinct jump in this case at the dynamic buckling load $\hat{\lambda} = 0.445$, see Figure 8b. A distinct jump also occurs for the mode (3, 5, 0), at $\hat{\lambda} = 0.415$, see Figure 8c. Similar to the phenomenon encountered in the example of Tamura's shell (Figure 4), already at lower loads a jump to the remote static branch may occur, corresponding to an escape through the unstable static equilibrium path to the remote static equilibrium path. For the deflection functions chosen, at the applied step loads $\hat{\lambda} = 0.385$ and $\hat{\lambda} = 0.388$ the shell buckles dynamically.

6. Concluding Remarks

A low-dimensional model has been presented that captures main characteristics of the dynamic stability and nonlinear flexural vibration behaviour of anisotropic cylindrical shells. The method is based on an

energy formulation using a small number of modes in combination with numerical time-integration of the resulting set of ordinary differential equations. The model makes it possible to perform parametrical studies for the three basic loading conditions, axial compression, radial pressure and torsion.

Results of the analysis have been compared with results from the literature. Characteristics of the dynamic buckling under axial step loading and vibration behaviour under axial parametric excitation have been demonstrated using this approach. The softening behaviour of shells under parametric excitation and the decrease in buckling load under step loading, as compared to the static case, have been illustrated.

The analysis presented may be extended to multi-mode analyses, which take the coupling between different circumferential and axial harmonics into account. This may be useful in particular for the topics of the present paper, dynamic buckling analyses and parametric excitation problems. To obtain an accurate simulation of the dynamic behaviour of practical shell structures it may further be necessary to use discretization models that include the effect of the boundary conditions at the shell edges, using a (one-dimensional or two-dimensional) finite difference or finite element scheme.

References

1. Herrmann, G. (ed.), *Dynamic Stability of Structures*, Pergamon Press, Oxford, 1967.
2. Bolotin, V. V., *The Dynamic Stability of Elastic Systems*, Holden-Day, San Francisco, California, 1963, translated by V.I. Weingarten et al..
3. Evan-Iwanowski, R., 'On the parametric resonance of structures', *Applied Mechanics Reviews* **18**(9), 1965, 699–702.
4. Hsu, C., 'On parametric excitation and snap-through stability problems of shells', in *Thin-Shell Structures – Theory, Experiment and Design*, Y. C. Fung and E. E. Sechler (eds.), Prentice-Hall, Englewood Cliffs, New Jersey, 1974, pp. 103–131.
5. Yao, J. C., 'Dynamic stability of cylindrical shells under static and periodic axial and radial loads', *AIAA Journal* **1**(6), 1963, 1391–1396.
6. Yao, J. C., 'Nonlinear elastic buckling and parametric excitation of a cylinder under axial loads', *ASME Journal of Applied Mechanics* **32**(1), 1965, 109–115.
7. Vijayaraghavan, A. and Evan-Iwanowski, R. M., 'Parametric instability of circular cylindrical shells', *ASME Journal of Applied Mechanics* **34**, 1967, 985–990.
8. Nagai, K. and Yamaki, N., 'Dynamic stability of circular cylindrical shells under periodic compressive forces', *Journal of Sound and Vibration* **58**(3), 1978, 425–441.
9. Argento, A., 'Dynamic stability of a composite circular cylindrical shell subjected to combined axial and torsional loading', *Journal of Composite Materials* **27**, 1993, 1722–1738.
10. Argento, A. and Scott, R., 'Dynamic instability of layered anisotropic circular cylindrical shells: Part I. Theoretical developments', *Journal of Sound and Vibration* **162**, 1993, 311–322.
11. Argento, A. and Scott, R., 'Dynamic instability of layered anisotropic circular cylindrical shells: Part II. Numerical results', *Journal of Sound and Vibration* **162**, 1993, 323–332.
12. Lindberg, H. E. and Florence, A. L., *Dynamic Pulse Buckling*, Martinus Nijhoff, Dordrecht, The Netherlands, 1987.
13. Simitses, G. J., *Dynamic Stability of Suddenly Loaded Structures*, Springer, New York, 1990.
14. Kounadis, A., 'Nonlinear dynamic buckling of discrete dissipative or nondissipative systems under step loading', *AIAA Journal* **29**, 1991, 280–289.
15. Budiansky, B. and Roth, R. S., 'Axisymmetric dynamic buckling of clamped shallow spherical shells', NASA TN D-1510, 1962.
16. Roth, R. and Klosner, J., 'Nonlinear response of cylindrical shells subjected to dynamic axial loads', *AIAA Journal* **2**, 1964, 1788–1794.
17. Tamura, Y. S. and Babcock, C. D., 'Dynamic stability of cylindrical shells under step loading', *ASME Journal of Applied Mechanics* **42**(1), 1975, 190–194.
18. Schokker, A., Sridharan, S., and Kasagi, A., 'Dynamic buckling of composite shells', *Computers & Structures* **59**(1), 1996, 43–53.
19. Saigal, S., Yang, T., and Kapania, R., 'Dynamic buckling of imperfection sensitive shell structures', *Journal of Aircraft* **24**, 1987, 718–724.

20. Ganapathi, M. and Varadan, T. K., 'Large amplitude vibrations of circular cylindrical shells', *Journal of Sound and Vibration* **192**(1), 1996, 1–14.
21. Tabiei, A., Tanov, R., and Simitses, G., 'Numerical simulation of cylindrical laminated shells under impulsive lateral pressure', *AIAA Journal* **37**(5), 1999, 629–633.
22. Ganapathi, M., Patel, B., and Sambandam, C., 'Parametric dynamic instability analysis of laminated composite conical shells', *Journal of Reinforced Plastics and Composites* **18**(14), 1999, 1336–1346.
23. Popov, A., Thompson, J., and McRobie, F., 'Low dimensional models of shell vibrations', *Journal of Sound and Vibration* **209**, 1998, 163–186.
24. Gonçalves, P. B. and Del Prado, Z. J. G. N., 'Nonlinear oscillations and stability of parametrically excited cylindrical shells', *Meccanica* **37**, 2002, 569–597.
25. Pellicano, F., Amabili, M., and Païdoussis, M. P., 'Effect of the geometry on the non-linear vibration of circular cylindrical shells', *International Journal of Non-Linear Mechanics* **37**(7), 2002, 1181–1198.
26. Pellicano, F. and Amabili, M., 'Stability and vibration of empty and fluid-filled circular cylindrical shells under static and periodic axial loads', *Journal of Solids and Structures* **40**, 2003, 3229–3251.
27. Amabili, M. and Païdoussis, M., 'Review of studies on geometrically nonlinear vibrations and dynamics of circular cylindrical shells and panels, with and without fluid-structure interaction', *Applied Mechanics Reviews* **56**(4), 2003, 349–381.
28. Liu, D. K., 'Nonlinear Vibrations of Imperfect Thin-Walled Cylindrical Shells', Ph.D. Thesis, Faculty of Aerospace Engineering, Delft University of Technology, The Netherlands, 1988.
29. Jansen, E. L., 'Non-stationary flexural vibration behaviour of a cylindrical shell', *International Journal of Non-Linear Mechanics* **37**(4/5), 2002, 937–949.
30. Brush, B. O. and Almroth, D. O., *Buckling of Bars, Plates and Shells*, McGraw-Hill, New York, 1975.
31. Jansen, E. L., 'Nonlinear Vibrations of Anisotropic Cylindrical Shells', Ph.D. Thesis, Faculty of Aerospace Engineering, Delft University of Technology, The Netherlands, 2001.
32. Khot, N. and Venkayya, V., 'Effect of fibre orientation on initial postbuckling behavior and imperfection sensitivity of composite cylindrical shell', Air Force Flight Dynamics Laboratory Technical Report-70-125, 1970.
33. Hearn, A. C., *REDUCE User Manual*, RAND, Santa Monica, California, 1993.
34. Booton, M., 'Buckling of Imperfect Anisotropic Cylinders under Combined Loading', UTIAS Report 203, Institute for Aerospace Studies, University of Toronto, 1976.
35. Bogdanovich, A., *Non-Linear Dynamic Problems for Composite Cylindrical Shells*, Elsevier, London, 1993.